Turkish Journal of Civil Engineering, 2024 87-102, Paper 763, ***Research Article***

A Quantitative Investigation on the Effects of Flexure-Dominated Reinforced Concrete Column Characteristics on the Dissipated Energy

Ziya MÜDERRISOĞLU[1*]
Ahmet Anıl DINDAR[2]
Ali BOZER[3]
Hasan ÖZKAYNAK[4]
Ahmet GÜLLÜ[5]
Bilal GÜNGÖR[6]
Furkan ÇALIM[7]
Serkan HASANOĞLU[8]

ABSTRACT

This paper presents the effects of fundamental member and loading parameters on total dissipated energy capacity of RC columns in a quantitative way by using an experimental database. Specifically, concrete compressive strength, yield strength of reinforcing bars; shear span-to-depth ratio, reinforcement ratios; peak drift ratio, and axial load ratio, are considered as influencing factors. Pearson's correlation coefficients are utilized as dependency indicators to construct a correlation matrix where the effect of each factor on

Note:
- This paper was received on March 28, 2023 and accepted for publication by the Editorial Board on October 13, 2023.
- Discussions on this paper will be accepted by May 31, 2024.
- https://doi.org/10.18400/tjce.1272125

1 Istanbul Beykent University, Department of Civil Engineering, Istanbul, Türkiye
ziyamuderrisoglu@beykent.edu.tr - https://orcid.org/0000-0003-1220-8047

2 Gebze Technical University, Department of Civil Engineering, Kocaeli, Türkiye
adindar@gtu.edu.tr - https://orcid.org/0000-0003-3168-8322

3 Eskişehir Technical University, Department of Civil Engineering, Eskişehir, Türkiye
alibozer@eskisehir.edu.tr - https://orcid.org/0000-0002-3632-2605

4 Istanbul Beykent University, Department of Civil Engineering, Istanbul, Türkiye
hasanozkaynak@beykent.edu.tr - https://orcid.org/0000-0003-2880-7669

5 Texas State University, Ingram School of Engineering, Texas, USA
ahmetgullu@txstate.edu - https://orcid.org/0000-0001-6678-9372

6 Gebze Technical University, Department of Civil Engineering, Kocaeli, Türkiye
bgungor@gtu.edu.tr - https://orcid.org/0000-0001-6749-2706

7 Istanbul Technical University, Faculty of Civil Engineering, Istanbul, Türkiye
calimf@itu.edu.tr - https://orcid.org/0000-0001-8365-9553

8 University School for Advanced Studies IUSS, Pavia, Italy
serkan.hasanoglu@iusspavia.it - https://orcid.org/0000-0002-7018-0479

* Corresponding author

dissipated energy level is quantified. Results show that the effective factors among selected features are peak drift ratio, transverse reinforcement volumetric ratios of a member, and yield strength of rebars whereas the heaviest influencing factors are the first two.

Keywords: Energy-based design, dissipated energy capacity, reinforced concrete columns, correlation levels.

1. INTRODUCTION

The fundamental structural design principle in earthquake engineering is to avoid failure of structural members and partial or total collapse of structural system. In other words, dissipating the earthquake-induced input energy without jeopardizing member integrity and structural stability is a key issue in seismic design. This is commonly achieved by maintaining adequate strength and ductility on material, section, and structural levels. Both the conventional seismic design procedures (i.e., force-based, and displacement-based), and recently developing design approach namely energy-based seismic design of structures, recommend the designers to avoid brittle or low-ductile behavior of components due to high compression forces; shear failure in members and connections; inadequate reinforcement development, splicing and development length. Once these actions are avoided, stable hysteresis loops, thus effective energy dissipation, through inelastic cyclic responses is achieved.

The inelastic cyclic response of structural members plays a crucial role in accumulation of deformations in a structure. When fundamental seismic design recommendations are improperly applied to a structural element, it can lead to misleading outcomes. This can result in the accumulation of damage throughout the structure, primarily caused by insufficient levels of total energy dissipation in individual structural members.

The energy dissipation capacity of the structural members is evaluated as calculating the area enclosed by the force-displacement hysteresis achieved during the cyclic loading. Specifically, the area under the force-displacement response is known as the dissipated energy. Examples of experiment-based loading procedure and corresponding component response are represented in Figures 1a and 1b, respectively [1].

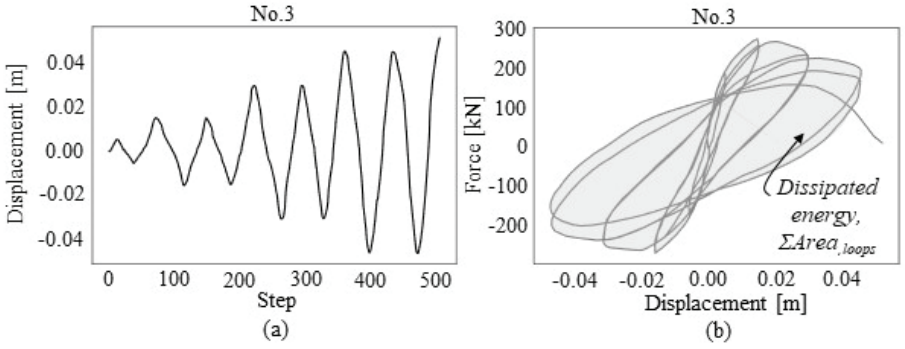

Figure 1 - (a) Experimental loading protocol, (b) obtained force-displacement hysteresis for No.3 specimen of Gill [1]

The prediction of component-based energy dissipation and deformation capacity has been studied by several researchers in the past years. Poljanšek et al. [2] presented the effects of fundamental input parameters on the hysteretic energy dissipation and deformation capacity of RC columns in terms of several normalized forms of energy quantities. They concluded that the hysteretic energy capacity is mostly affected by the reinforcement ratio and axial load level variations. Acun and Sucuoglu [3] investigated the effect of failure modes, ductility, and material characteristics of RC columns on the energy dissipation capacity. For this purpose, test units were subjected to cyclic displacements having varying amplitudes. Deteriorations were observed in dissipated energy levels with constant-amplitude cycle numbers. Rodrigues et al. [4] performed an experimental study to assess the energy dissipation characteristics and to estimate the equivalent damping ratio of RC columns under biaxial bending effects via full-scale testing. Significant variations in dissipated energy capacity were observed due to the level of axial loading. Vu et al. [5] investigated the effects of variability in axial loads on the hysteresis characteristics of RC short columns. Results showed that the hysteresis loops become more unsymmetrical depending on the variations in axial load. Yang et al. [6] performed an experimental study to reveal the effects of the corrosion of rebars on hysteresis behavior. Critical thresholds for the maximum corrosion level and numerical dilation crack widths were proposed. Based on component-based investigations detailed as above, recently proposed seismic design methodologies are being developed to implement the energy-based design principles for RC type structures [7].

Due to the limitations in the number of specimens that can be tested, researchers may also refer to the existing experimental databases [8-10]. Very often, these databases are compiled based on specimen and reinforcement details, test loading protocols and types. Then, the compiled datasets are either used to investigate the correlations between the feature and target quantities or to propose empirical equations for predicting the target parameter [11-12]. Finally, relevant research studies may be a good basis for defining the hysteresis rules in scope of analytical processes [13-16].

The attention on the energy-based seismic design is increasing, however, determination of the energy capacity of structural members and joints is still a developing topic. To the authors' knowledge, even here are numerous efforts on predicting the energy dissipation capacities that will contribute to the improved design of structural members [17-20], very limited or none of them deals with predicting the effects of parameters on energy dissipation capacities in a quantitative way. Hence, the rationale of this study is to associate the section and loading characteristics with the dissipated energy levels of members and thus to release crucial impact on energy capacity of RC columns. Moreover, a fore-knowledge of influencing factors may lead the designers to more efficient solutions and may provide a basis for future seismic code provisions focusing on the energy-based design concept. Specifically, the correlations are revealed in a quantitative way with the compilation of a dataset. For this purpose, the compiled dataset is described first, and the statistical properties are given. Then, the methods to be used for correlation-based investigations are explained. Following the discussions for the correlation and dependency levels between the features and target capacity parameter, selected test unit characteristics are further investigated. In this paper, the target dataset is fundamentally focused on flexure-dominated rectangular RC column type members to represent new code compliant structures. In the study, a wide feature parameter set, (i.e., concrete compressive strength, yield strength of rebars, shear span-to-depth ratio, longitudinal rebar ratio -as the ratio between the area of longitudinal rebars and the member

cross-sectional area- and transverse reinforcement volumetric ratios -as the ratio between the volume of transverse reinforcement spaced as the interval and the core area times spacing between transverse reinforcement-, peak drift ratio, and axial load ratio) were considered. The effect of shear deformations on the shape of hysteresis loops are not considered within the scope of this work but based on this premise, further investigations will be implemented into different database contents by taking into account the proposed procedure.

2. MATERIAL AND METHODOLOGY

Details of compiled test unit database and methods that are used to investigate the dependency levels between the selected features and energy capacity parameters are explained in this section.

2.1. RC Column Test Unit Database

Open access databases provide a basis for analytical studies including metadata and the responses of past experiments in the literature as verification results. The database used in this study is extracted from DesignSafe database [9] that includes RC column test units having rectangular type cross-sections that are subjected to flexural effects. In this study, the authors emphasized the importance of assembling a dataset that accurately reflects the scope of their research. They compiled RC column information from existing databases, specifically focusing on rectangular cross sections subjected to flexural effects. However, they discovered that approximately 37% of the dataset (24 out of 65 specimens) had almost identical metadata characteristics obtained from a single reference. The presence of a large number of data representing similar characteristics may introduce a bias in the results, therefore these data were eliminated. Moreover, it was also observed that the remaining limited data basically represent the commonly considered member characteristics in existing buildings. Selected criteria are given in Table 1. Here, the axial load ratio refers to the ratio between the axial load acting on a member during the test and the cross-sectional area, and the material strengths are considered as nominal values reported for a test unit. After filtering the compiled dataset by taking into account the criteria, the 41 test units subjected to static reversed cyclic loadings is set for the analysis.

Table 1 - Selection criteria and limitations for the compiled dataset

Feature	Limitation
Compressive strength of concrete, f_c [MPa]	≤ 45
Yield strength of longitudinal rebar, f_{yl} [MPa]	≤ 500
Yield strength of transverse rebar, f_{yt} [MPa]	≤ 500
Shear span-to-depth ratio, a/d	≥ 3
Axial load ratio, ρ_{axial}	Between 0.15 and 0.40

Identified critical properties which predominantly influence hysteretic behavior thus energy dissipation, and their respective relative frequencies within the dataset are given in Figure 2. Moreover, the statistical parameters for selected features are provided in Table 2.

Table 2 - Statistical parameters of the selected features and target response

Parameter/ Indicator	f_c [MPa]	f_{yl} [MPa]	f_{yt} [MPa]	a/d [-]	ρ_l [-]	ρ_t [-]	Δ_{max} [-]	ρ_{axial} [-]	E_{cd} [kNm]
Minimum	17.6	330.9	254.9	3.28	0.0101	0.0016	0.018	0.15	2.94
Maximum	44.0	496.9	475.9	8.9	0.0382	0.0300	0.102	0.39	597.93
Median	27.1	439.9	391.9	4.1	0.0194	0.0148	0.051	0.22	66.42
Mean	29.1	433.4	395.7	4.6	0.0208	0.0149	0.053	0.23	154.29
Skew	1.08	-0.67	-0.30	1.64	1.08	0.21	0.22	0.63	1.34

ρ_l: Longitudinal rebar ratio, ρ_t: Transverse rebar volumetric ratio, Δ_{max}: Peak drift ratio, E_{cd}: Total dissipated energy

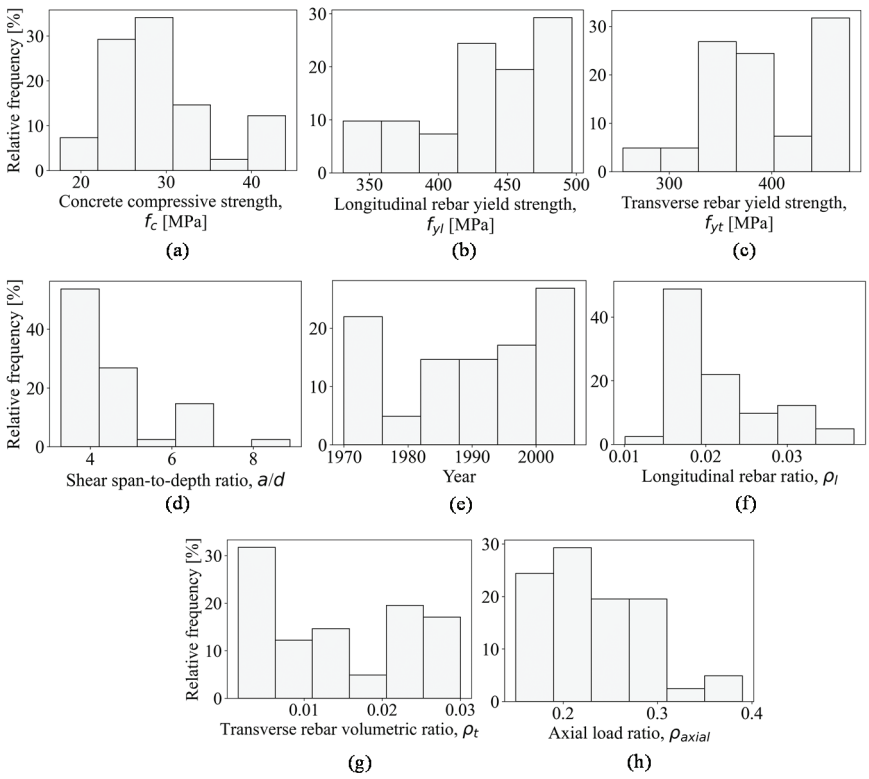

Figure 2 - Relative frequency distributions of fundamental properties for a selected dataset: (a) f_c, (b) f_{yl}, (c) f_{yt}, (d) a/d, (e) test year, (f) ρ_l, (g) ρ_t, (h) ρ_{axial}.

The cumulative energy dissipation and corresponding total dissipated energy capacities of selected test units are represented in Figure 3. The total energy dissipation capacity of the columns is determined as the area enclosed by the base shear and top displacement hysteresis derived through the entire experiment. In Figure 3a, development of the cumulative energy dissipation through the increasing steps for each specimen is illustrated whereas the total energy dissipation capacities of the specimens are given in Figure 3b. Numerical values of the input features of the test units considered in this study are provided in Appendix/Table A.1.

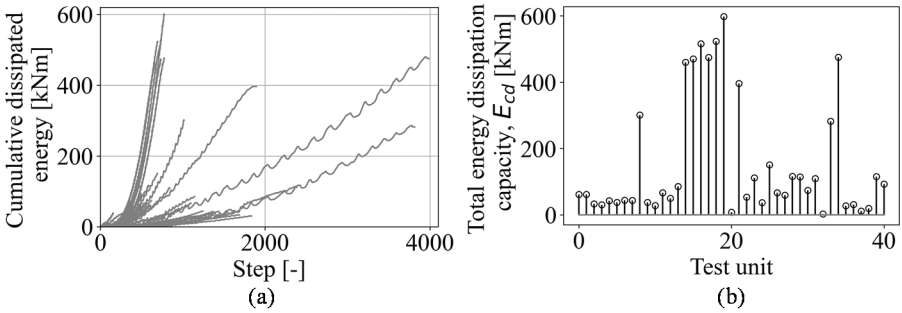

Figure 3 - Variabilities on the dissipated energy levels of selected test units: (a) cumulative energy dissipations, (b) total energy dissipation capacities

Based on a compilation of the dataset, the correlations between the selected features and the target total energy dissipation capacities are investigated next by considering a statistical approach (i.e., using the Pearson's correlation coefficient [21]).

2.2. Dependency of the Dissipated Energy Capacity on Selected Features

The dissipated energy is used to quantitatively represent the cumulative damage level since the seismic energy is the enclosed area by force-displacement relation of each column. Thereby, correlation of the damage on the columns with a scalar quantity, i.e., energy, is possible.

Here, the minimum and the maximum dissipated energies were obtained as 2.94 kNm and 597.93 kNm, respectively. The variation of energy capacities is directly related to several factors, including the sectional/geometrical, material, and mechanical properties of test units, as well as the loading path characteristics. Previous research [2,11] has shown that selected parameters have a significant impact on the dissipated energy capacity. However, there are additional parameters, such as peak drift ratio and yield strength of rebars, that are directly implemented to enhance the features for a more comprehensive analysis.

In the current study, the dependency level of dissipated energy capacity on selected features is investigated by using the correlation between the input and target parameters. For this purpose, the Pearson's correlation coefficients are considered as dependency indicators. Following equation is implemented to predict the level of correlation:

$$\rho_{F,T} = \frac{\sigma_{FT}}{\sigma_F \sigma_T} \quad (1)$$

Here, σ_{FT} is the covariance between the selected feature and the target response, and σ_F and σ_T denote for the standard deviations of feature and target data, respectively. Here, the implemented parametric correlation approach enables user to measure the level of linear dependence between two variables based on distribution characteristics.

3. STATISTICAL INVESTIGATION

Predicted correlation levels are presented as heatmaps by utilizing the Python [22,23] software. In Figure 4, the correlations between the selected feature set and the energy capacity levels are presented. In this matrix, the boundary levels of +1, 0, and -1 of a correlation matrix typically represent the complete positive, no correlation, and complete negative correlation levels, respectively. Here, the complete positive correlation case basically corresponds to a directly proportional relationship between the selected feature and the target parameter (i.e., as target parameter increases the feature level also increases by the exactly same percentage). An exactly opposite relationship between two variables is observed in case of a complete negative correlation. It is observed from the figure that, loading characteristics (i.e., axial load ratio and peak drift ratio) and transverse rebar properties have considerable effects on the dissipated energy. Specifically, the peak drift ratio and the transverse reinforcement contribute the total dissipated energy capacity, mostly (i.e., as moderate positive correlation levels of 0.60, approximately). However, it should be noted that this case is especially valid for well-confined (i.e., by considering the maximum reinforcement ratio recommendations available in codes and standards) sections. The correlation between the concrete material characteristics and the energy capacity is lower compared to those correlation levels of other features. Here, it should be noted that only 4 out of 41 total test specimens' concrete compressive strength levels are not considered as normal strength concrete (e.g., 20 MPa < f_c < 40 MPa). A comprehensive comparison for the effect of normal and high-strength concrete RC columns concluded that the total energy dissipation capacity of normal strength concrete is higher than that of the capacity of high strength concrete because of the brittle nature of high strength concrete. This can be attributed to the fact that the inverse relationship between strength and the ductility level of material affects the dissipated energy levels [2].

The levels of individual correlations are summarized in Figure 5. The results show that, the total dissipated energy capacity is mostly influenced by the peak drift ratio. The total dissipation capacity increases with an increasing peak drift ratio. This indicates that although strength degradation due to high level damage state occurs, members still dissipate energy which might be called residual capacity. On the other hand, an opposite trend is valid for the axial load level. Figure 5 shows that, for test specimens subjected to lower axial load levels have higher energy capacity. The total energy dissipation capacity decreases due to high axial stress levels owing to the specimens' lateral deformation is limited under the effects of high axial loads. Comparison over the material characteristics reveals that, rebar yield strength positively influences dissipated energy capacity of the member. Based on ductile design principle, it is also observed that high dissipated energy capacities are obtained for heavily reinforced test specimens (i.e., a positive correlation level of 0.53) and well-confined sections. As the dataset selected in this study includes flexure-dominated RC column type

test units, the minimum threshold for shear span-to-depth ratios is limited by 3. Due to this limitation, an increment trend in energy capacity is observed for decreasing values of shear span-to-depth ratios (i.e., a negative correlation level of -0.3). This inverse proportionality trend for other case (i.e., for $a/d < 3$ RC columns) was recommended in previous studies [2]

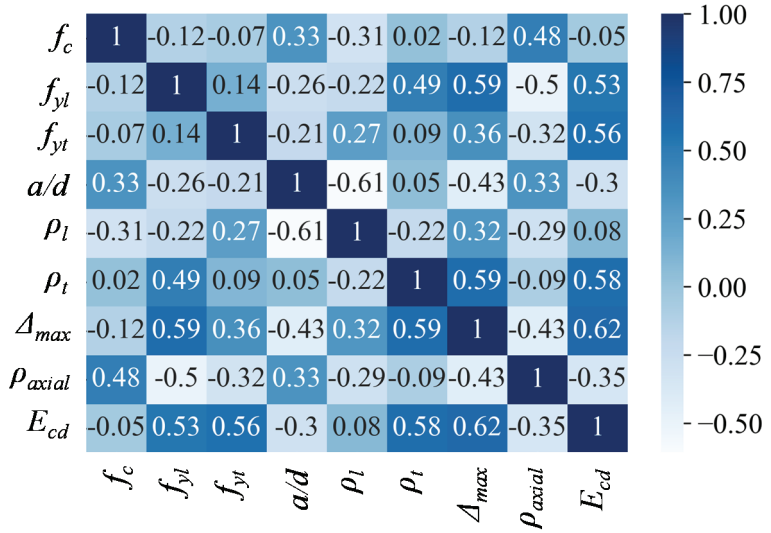

Figure 4 - Correlation matrix for input features and the dissipated energy level

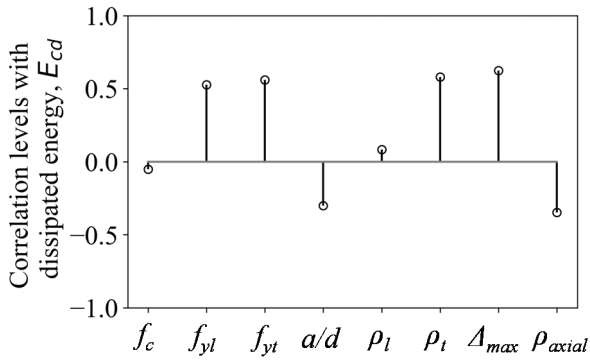

Figure 5 - Correlation with dissipated energy levels obtained for input features

The pairwise regression plots with 95% of confidence intervals for a single feature (i.e., peak drift ratio) having the highest positive correlation with the dissipated energy capacity, and for the opposite case such as axial load ratio that shows a considerable negative correlation with the target parameter, are given in Figures 6a and 6b, respectively. Moreover, additional partial figures given at top and right of the figure of interest represent the approximate feature distribution and tendency characteristics.

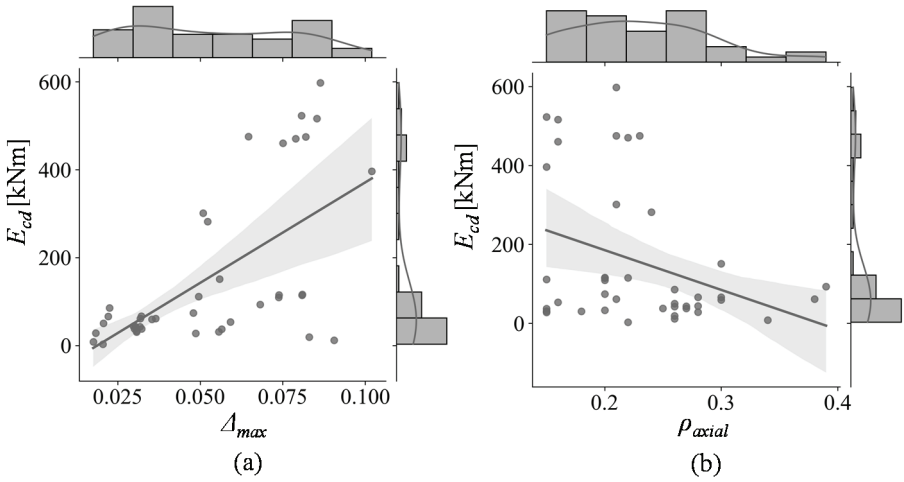

Figure 6 - Pairwise regression between: (a) Δ_{max} -E_{cd} , (b) ρ_{axial} -$E_{cd.}$

In order to compare the energy dissipation characteristics of RC column test units having the minimum (i.e., UM_205 [24]) and the maximum (i.e., C3-3 [25]) energy capacities in a dataset, the total dissipated energy, $E_{cd,L}$ normalized by the maximum strength, F_{max} and the shear span a is given as follows:

$$E_{cd,L} = \frac{E_{cd}}{F_{max} \times a} \tag{2}$$

General properties and loading histories of the test units UM_205 and C3-3 are provided in Table 3 and Figures 7a and 7b.

Table 3 - General properties of test units

ID	Year	Δ_{max}	ρ_t	ρ_{axial}	a/d	f_{yt} [MPa]
UM_ 205	1970	0.021	0.003	0.22	3.3	324.1
C3-3	2000	0.086	0.006	0.21	4	459.4

Regarding the general characteristics provided in Table 3, the fundamental differences between test specimens are mainly based on the transverse rebar amount, its material quality, and peak displacement properties. The normalized energy dissipation capacities are compared by considering the elastic (1), pre-capping (2), and post-capping (3) regions (Figures 8a and 8b). While the hysteretic curves of the specimens were given by solid lines, the envelope of the hysteresis loops are given by dashed lines in the figures.

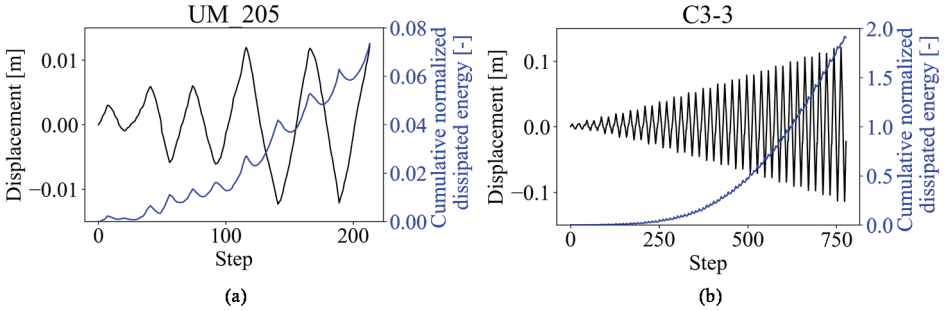

Figure 7 - Loading histories of test specimens: (a) UM_205, (b) C3-3

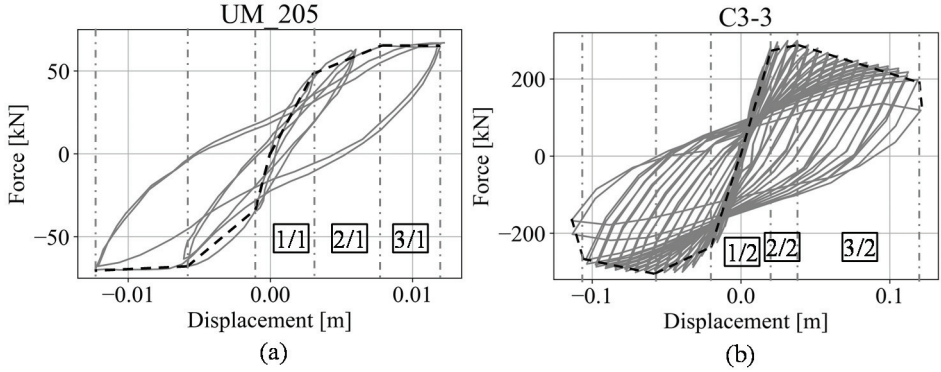

Figure 8 - Force-displacement history and envelopes for test specimens:(a) UM_205, (b) C3-3

The preliminary results indicate that, the highest amount of energy is dissipated at post-capping regions for UM-205 and C3-3 test units (i.e., 69.4% and 88.7% of total dissipated energy, respectively). Moreover, it is seen that in the post-capping region, normalized dissipated energy graph has a steeper slope for the C3-3 test unit (Figure 9). This is attributed to both the strong level of correlated features (Table 3), and the large number of cycles captured during the loading stages for C3-3 test specimen. Further clarification can be achieved by investigating the related issue.

The correlation levels are also investigated by using the normalized capacity for the entire data set. Similar observations with the total energy dissipation capacity-based results, are obtained for the selected indicator (Figure 10a). Moreover, to compare the calculated correlation levels via total and normalized dissipated energy levels, the relative differences between the two approaches are compared (Figure 10b). Here, the positive relative differences indicate an increment in predicted correlation level by implementing the normalized energy capacity parameters in dependency-based investigations. Specifically, even similar trends are obtained for both approaches, the correlation level between the high-

correlated features and the target capacity may be also increased (i.e., correlation level for transverse reinforcement ratio is 0.58 to 0.71 from approximately moderate to strong positive correlation).

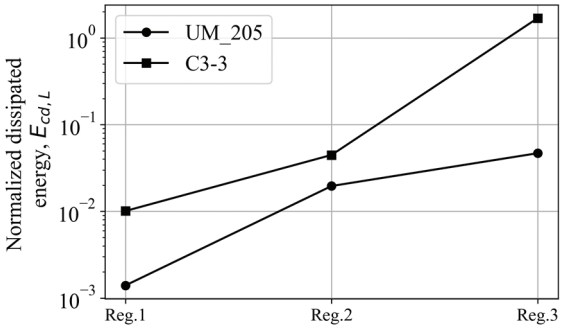

Figure 9 - Comparison of normalized dissipated energy capacities

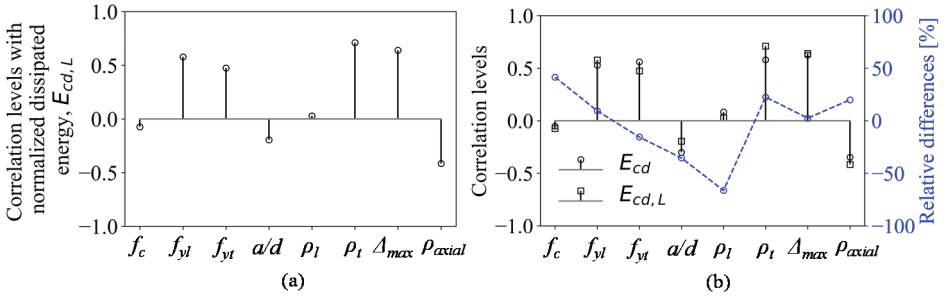

Figure 10 - (a) Correlation levels obtained for input features using the normalized capacity parameter, (b) Comparison between two capacity indicators

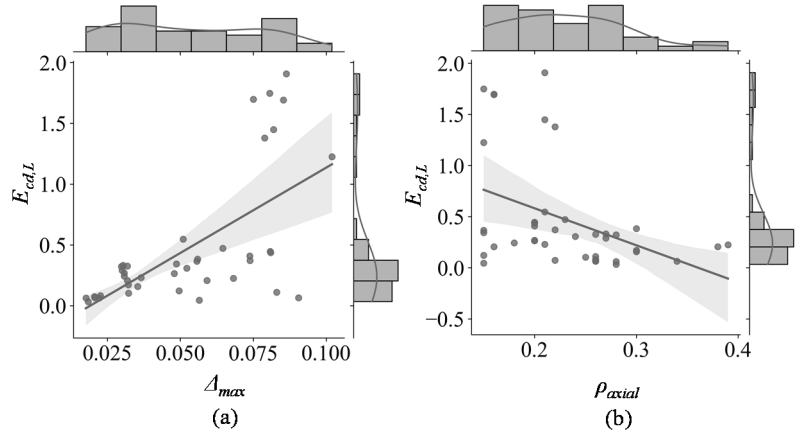

Figure 11 - Pairwise regression between: (a) Δ_{max} -$E_{cd,L}$, (b) ρ_{axial} -$E_{cd,L}$.

Finally, to compare the input feature-based results between the total dissipated energy and the normalized parameter evaluated through Equation 2, the pairwise regression plots for peak drift ratio and the axial load ratio are given in Figures 11a and 11b, respectively. Similar to the overall regression trends captured for total dissipated energy capacities, the positive and negative correlations are also observed for selected input features.

4. DISCUSSION AND CONCLUSION

A quantitative investigation of the effects of flexure-dominated RC column properties on the total energy dissipation capacity is presented and discussed in this paper. For this purpose, a dataset including 41 RC column test units is compiled from the existing comprehensive databases. Correlations between the selected fundamental member and loading-base features and the dissipated energy capacity parameter are represented using the commonly used statistical approaches. Results of the study are summarized below:

- The degree of dependency of the energy capacity on critical features is obtained numerically. For this purpose, a considerable number of a parameter set (i.e., 8 parameters) is considered. Peak drift ratios and the axial load levels are found to have the highest positive and negative correlations, respectively.
- For flexure-dominated RC columns, a negative correlation is obtained between the shear span-to-depth ratio and the dissipated energy capacity parameter which indicates that shear-domination has negative affect on the member response.
- Higher energy dissipation capacity levels are obtained for well-confined members. It is found that this is directly proportional to the volumetric ratio of transverse reinforcement.
- It is observed that the minimum concrete strength and longitudinal rebar ratio have a marginal effect on the dissipated energy capacity.
- In order to consider the possible effects of dispersions due to member-wise characteristics, the correlation levels are also calculated via normalized dissipated energy capacity parameter. Similar trends in dependencies are also obtained for the actual and normalized capacity levels.

As energy-based seismic design of structures gains popularity, the metadata including a detailed experimental information of existing test specimens compiled using the available databases in the literature may be a good starting point for future analytical studies. Moreover, correlation levels evaluated in the current study are believed to have a contribution to future seismic codes that include the fundamentals of energy-based design procedures by taking into account the effectiveness levels of structural member related features in a statistical way. In other words, the outcomes of this study are essential for use in implicit equations, which may aim to estimate the energy dissipation capacity of structural elements and the proposed methodology could be extended to determine the energy dissipation capacity of dual systems and/or moment resisting frame systems containing beam, shear wall and column elements. Additionally, the study provides insights into the critical features that affect the energy dissipation capacity of these members, which can be considered in the design process. The outcomes can be used to calibrate current design standards and practices for assessing the seismic performance of buildings with configuration irregularities in terms

of providing quantitative triggers and related design requirements that can be used to improve the seismic performance of buildings.

Acknowledgment

This work has been funded and supported by the Scientific and Technological Research Council of Türkiye, (TÜBİTAK, Turkish Research Foundation), Project ID: 121M713. This support is greatly acknowledged.

References

[1] Gill, W.D., Ductility of Rectangular Reinforced Concrete Columns with Axial Load. University of Canterbury, Department of Civil Engineering, Master of Engineering, 1979.

[2] Poljanšek, K., Peruš, I., Fajfar, P., Hysteretic Energy Dissipation Capacity and the Cyclic to Monotonic Drift Ratio for Rectangular RC columns in Flexure. Earthquake Engineering & Structural Dynamics, 38(7), 2009.

[3] Acun, B., Sucuoğlu, H., Energy Dissipation Capacity of Reinforced Concrete Columns under Cyclic Displacements. ACI Structural Journal, 109(4), 2012.

[4] Rodrigues, H., Furtado, A., Arêde, A., Behavior of Rectangular Reinforced-Concrete Columns Under Biaxial Cyclic Loading and Variable Axial Loads. Journal of Structural Engineering, 142(1), 04015085, 2016.

[5] Vu, N.S., Li, B., Tran, C.T.N., Seismic Behavior of Reinforced Concrete Short Columns Subjected to Varying Axial Load. ACI Structural Journal, 119(6), 2022.

[6] Yang, S. Y., Song, X. B., Jia, H. X., Chen, X., Liu, X. L., Experimental Research on Hysteretic Behaviors of Corroded Reinforced Concrete Columns with Different Maximum Amounts of Corrosion of Rebar. Construction and Building Materials, 121, 2016.

[7] Yalçın, C., Dindar, A. A., Yüksel, E., Özkaynak, H., Büyüköztürk, O., Seismic Design of RC Frame Structures based on Energy-Balance Method. Engineering Structures, 237, 112220, 2021.

[8] Browning, J.A., Pujol, S., Eigenmann, R., Ramirez, J.A., NEEShub Databases. Concrete International, https://datacenterhub.org/resources/databases, 2013 (Accessed: 01.10.2021).

[9] Rathje, E., Dawson, C. Padgett, J.E., Pinelli, J.-P., Stanzione, D., Adair, A., Arduino, P., Brandenberg, S.J., Cockerill, T., Dey, C., Esteva, M., Haan, Jr., F.L., Hanlon, M., Kareem, A., Lowes, L., Mock, S., Mosqueda, G., DesignSafe: A New Cyberinfrastructure for Natural Hazards Engineering. ASCE Natural Hazards Review, 18(3), 2017.

[10] Berry, M., Parrish, M., Eberhard, M., PEER structural performance database user's manual (version 1.0). University of California, Berkeley, 2004.

[11] Haselton, C.B., Assessing Seismic Collapse Safety of Modern Reinforced Concrete Moment Frame Buildings, Stanford University, Doctoral Dissertation, 2006.

[12] Liu, Z., Wang, Y., Cao, Z., Chen, Y., Hu, Y., Seismic Energy Dissipation Under Variable Amplitude Loading for Rectangular RC Members in Flexure. Earthquake Engineering & Structural Dynamics, 47(4), 2018.

[13] Ibarra, L. F., Medina, R. A., Krawinkler, H., Hysteretic Models that Incorporate Strength and Stiffness Deterioration. Earthquake Engineering & Structural Dynamics, 34(12), 2005.

[14] Di Domenico, M., Ricci, P., Verderame, G. M., Empirical Calibration of Hysteretic Parameters for Modelling the Seismic Response of Reinforced Concrete Columns with Plain Bars. Engineering Structures, 237, 112120, 2021.

[15] Rodas, P. T., Zareian, F., Kanvinde, A., Hysteretic Model for Exposed Column–Base Connections. Journal of Structural Engineering, 142(12), 04016137, 2016.

[16] Horton, T. A., Hajirasouliha, I., Davison, B., Ozdemir, Z., Accurate Prediction of Cyclic Hysteresis Behaviour of RBS Connections Using Deep Learning Neural Networks. Engineering Structures, 247, 113156, 2021.

[17] Rayjada, S. P., Raghunandan, M., Ghosh, J., Machine Learning-Based RC Beam-Column Model Parameter Estimation and Uncertainty Quantification for Seismic Fragility Assessment. Engineering Structures, 278, 2023.

[18] Luo, H., Paal, S. G., Machine Learning–Based Backbone Curve Model of Reinforced Concrete Columns Subjected to Cyclic Loading Reversals. Journal of Computing in Civil Engineering, 32(5), 2018.

[19] Akbaş, B., Jay, Shen, Depreme Dayanıklı Yapı Tasarımı ve Enerji Kavramı. Teknik Dergi, 14(67), 2003.

[20] Merter, O., Bozdağ, Ö., Düzgün, M., Energy-based Design of Steel Structures According to the Predefined Interstory Drift Ratio, Teknik Dergi, 23(115), 1573-1593, 2012.

[21] Pearson, K., Notes on the history of correlation. Biometrika, 13(1), 25-45, 1920.

[22] Van Rosum, G., Drake, F.L., Python 3 reference manual, CreateSpace, 2009.

[23] Waskom, M.L., Seaborn: Statistical Data Visualization. Journal of Open Source Software, 6(60), 2021.

[24] Umemura H., Endo, T., Report by Umemura Lab, Tokyo University, 1970.

[25] Mo, Y. L., Wang, S. J., Seismic Behavior of RC Columns with Various Tie Configurations. Journal of Structural Engineering, 126(10), 1122-1130, 2000.

[26] Atalay, M. B., Penzien, J., The Seismic Behavior of Critical Regions of Reinforced Concrete Components as Influenced by Moment, Shear and Axial Force. Berkeley, CA, USA: Earthquake Engineering Research Center, University of California, 1975.

[27] Harries, K. A., Ricles, J. R., Pessiki, S., Sause, R., Seismic Retrofit of Lap Splices in Nonductile Square Columns Using Carbon Fiber-Reinforced Jackets. ACI Structural Journal, 103(6), 874, 2006.

[28] Lynn, A. C., Moehle, J. P., Mahin, S. A., Holmes, W. T., Seismic Evaluation of Existing Reinforced Concrete Building Columns. Earthquake Spectra, 12(4), 715-739, 1996.

[29] Nosho, K., Stanton, J., MacRae, G., Retrofit of Rectangular Reinforced Concrete Columns Using Tonen Forca Tow Sheet Carbon Fiber Wrapping. Report No. SGEM, 96-2, 1996.

[30] Saatcioglu, M., Ozcebe, G., Response of Reinforced Concrete Columns to Simulated Seismic Loading. Structural Journal, 86(1), 3-12, 1989.

[31] Sezen, H., Moehle, J. P., Seismic Behavior of Shear-Critical Reinforced Concrete Building Columns. In Seventh US National Conference on Earthquake Engineering, Earthquake Engineering Research Institute, Boston, MA, 2002.

[32] Soesianawati, M. T., Limited Ductility Design of Reinforced Concrete Columns, 1986.

[33] Tanaka, H., Park, R., Effect of Lateral Confining Reinforcement on the Ductile Behavior of Reinforced Concrete Columns [Report 90-2]. Department of Civil Engineering, University of Canterbury, 1990.

[34] Wehbe, N., Saiidi, M.S., Sanders, D., Confinement of Rectangular Bridge Columns for Modrate Seismic Areas. National Center for Earthquake Engineering Research, 1998.

[35] Wight, J. K., Sozen, M. A., Shear Strength Decay in Reinforced Concrete Columns Subjected to Large Deflection Reversals. Structural Research Series No. 403. Civil Engineering Studies. Urbana-Champaign (IL): University of Illinois, 1973.

[36] Yoshimura, M. Y., Ultimate Limit State of RC Columns. The Second U.S.- Japan Workshop on Performance-Based Earthquake Engineering Methodology, 2000.

[37] Zahn, F. A., Priestley, M.J.N., Design of Reinforced Concrete Bridge Columns for Strength and Ductility. Christchurch, New Zealand, University of Canterbury, 1986.

APPENDIX

Table A.1 - Input features and total energy dissipation capacities of the test units considered in this study

ID	Unit	Ref.	bxh** [m]	H* [m]	ρ_{axial} [-]	f_c [MPa]	f_{yl} [MPa]	f_{yt} [MPa]	a/d [-]	ρ_l [-]	ρ_t [-]	E_{cd} [kNm]
1	No.3	[1]	0.40x0.40	1.60	0.38	23.6	426.9	320.0	4.50	0.0151	0.0280	61.46
2	No.4	[1]	0.40x0.40	1.60	0.21	25.0	426.9	280.0	4.45	0.0151	0.0220	61.47
3	No.5S1	[26]	0.31x0.31	1.68	0.20	29.4	428.9	391.9	6.64	0.0163	0.0150	33.33
4	No.6S1	[26]	0.31x0.31	1.68	0.18	31.8	428.9	391.9	6.64	0.0163	0.0090	30.53
5	No.9	[26]	0.31x0.31	1.68	0.26	33.3	362.9	391.9	6.64	0.0163	0.0150	42.82
6	No.10	[26]	0.31x0.31	1.68	0.27	32.4	362.9	391.9	6.64	0.0163	0.0090	37.96
7	No.11	[26]	0.31x0.31	1.68	0.28	31.0	362.9	372.9	6.64	0.0163	0.0150	44.02
8	No.12	[26]	0.31x0.31	1.68	0.27	31.8	362.9	372.9	6.64	0.0163	0.0090	43.29
9	NC1	[26]	0.46x0.46	1.37	0.21	39.3	438.9	453.9	3.49	0.0194	0.0220	301.15
10	L0	[27]	0.46x0.46	2.40	0.25	24.6	459.9	437.8	5.88	0.0148	0.0020	37.64
11	2CMH18	[28]	0.46x0.46	2.95	0.28	25.5	330.9	399.8	3.71	0.0194	0.0016	28.45
12	3SMD12	[28]	0.46x0.46	2.95	0.28	25.5	330.9	399.9	3.74	0.0303	0.0041	66.42
13	3CMH18	[28]	0.46x0.46	2.95	0.26	27.6	330.9	399.8	3.74	0.0304	0.0016	50.33
14	3CMD12	[28]	0.46x0.46	2.95	0.26	27.6	330.9	399.8	3.74	0.0304	0.0042	85.68
15	C1-2	[25]	0.40x0.40	1.40	0.16	26.7	496.9	459.4	4.00	0.0214	0.0300	460.46
16	C1-3	[25]	0.40x0.40	1.40	0.22	26.1	496.9	459.4	4.00	0.0214	0.0300	470.45
17	C2-2	[25]	0.40x0.40	1.40	0.16	27.1	496.9	459.4	4.00	0.0214	0.0300	516.26
18	C2-3	[25]	0.40x0.40	1.40	0.21	26.8	496.9	459.4	4.00	0.0214	0.0300	475.05
19	C3-2	[25]	0.40x0.40	1.40	0.15	27.5	496.9	459.4	4.00	0.0214	0.0300	523.20
20	C3-3	[25]	0.40x0.40	1.40	0.21	26.9	496.9	459.4	4.00	0.0214	0.0300	597.93
21	No.1	[29]	0.28x0.28	2.13	0.34	40.6	406.9	350.9	8.90	0.0101	0.0218	8.15
22	U4	[30]	0.35x0.35	1.00	0.15	32.0	437.9	469.9	3.28	0.0331	0.0250	396.52
23	U2	[30]	0.35x0.35	1.00	0.16	30.2	452.9	469.9	3.28	0.0321	0.0069	53.62
24	Specimen_1	[31]	0.46x0.46	2.95	0.15	21.1	434.3	475.9	3.76	0.0248	0.0020	111.65
25	Specimen_4	[31]	0.46x0.46	2.95	0.15	21.8	434.3	475.9	3.76	0.0248	0.0020	37.35
26	No.2	[32]	0.40x0.40	1.60	0.30	44.0	445.9	359.9	4.31	0.0151	0.0120	151.02
27	No.3	[32]	0.40x0.40	1.60	0.30	44.0	445.9	363.9	4.30	0.0151	0.0080	66.57
28	No.4	[32]	0.40x0.40	1.60	0.30	40.0	445.9	254.9	4.29	0.0151	0.0060	59.70
29	No1	[33]	0.40x0.40	1.60	0.20	25.6	473.9	332.9	4.73	0.0157	0.0250	116.28
30	No2	[33]	0.40x0.40	1.60	0.20	25.6	473.9	332.9	4.73	0.0157	0.0250	114.47
31	No3	[33]	0.40x0.40	1.60	0.20	25.6	473.9	332.9	4.73	0.0157	0.0250	74.14
32	No4	[33]	0.40x0.40	1.60	0.20	25.6	473.9	332.9	4.73	0.0157	0.0250	109.45
33	UM_205	[24]	0.20x0.20	0.60	0.22	17.6	462.0	324.1	3.33	0.0199	0.0061	2.94
34	A2	[34]	0.38x0.61	2.34	0.24	27.2	447.9	427.9	4.12	0.0222	0.0040	282.08
35	B2	[34]	0.38x0.61	2.34	0.23	28.1	447.9	427.9	4.10	0.0222	0.0050	475.25
36	WI_40_048E	[35]	0.15x0.31	0.88	0.15	26.1	495.9	344.9	3.45	0.0245	0.0048	27.76
37	WI_40_048W	[35]	0.15x0.31	0.88	0.15	26.1	495.9	344.9	3.45	0.0245	0.0048	31.35
38	FS0	[36]	0.30x0.30	0.90	0.26	27.0	386.9	354.9	3.53	0.0382	0.0148	11.92
39	FS1	[36]	0.30x0.30	0.90	0.26	27.0	386.9	354.9	3.53	0.0382	0.0148	19.33
40	No.7	[37]	0.40x0.40	1.60	0.22	28.3	439.9	465.9	4.34	0.0151	0.0160	115.26
41	No.8	[37]	0.40x0.40	1.60	0.39	40.1	439.9	465.9	4.34	0.0151	0.0200	93.18

* H: Height of test unit; b,h: Column cross-sectional dimensions along and perpendicular to loading, respectively.